



## 15 **Abstract**

16 Understanding past changes in precipitation extremes could help us predict their dynamics under  
17 future conditions. We present a novel approach for analyzing trends in extremes and attributing  
18 them to changes in the local precipitation regime. The approach relies on the separation between  
19 intensity distribution and occurrence frequency of storms. We examine the relevant case of the  
20 eastern Italian Alps, where significant trends in annual maximum precipitation over the past  
21 decades were observed. The model is able to reproduce observed trends at all durations between  
22 15 minutes and 24 hours, and allows to quantify trends in extreme return levels. Despite the  
23 significant increase in storms occurrence and typical intensity, the observed trends can be only  
24 explained considering changes in the tail heaviness of the intensity distribution, that is the  
25 proportion between heavy and mild events. Our results suggest these are caused by an increased  
26 proportion of summer convective storms.

## 27 **Plain Language Summary**

28 Quantifying past trends in extreme rainfall is important because it can help us understand future  
29 changes caused by global warming. Climate scientists and hydrologists use specific statistical  
30 models to do so, but interpreting the results is complicated because extremes are rare and the  
31 structure of the models is not linked to the local meteorology. We use a new statistical model that  
32 allows to better understand the mechanisms behind the trends we detect. We find that extreme  
33 rainfall in the eastern Italian Alps increased over the past decades and we associate this change to  
34 an increased proportion of summer thunderstorms.

## 35 **1 Introduction**

36 Understanding past and future changes in extreme subdaily precipitation intensities is of  
37 enormous interest because they are responsible for flash floods, urban floods, landslides and  
38 debris flows, and cause numerous casualties and huge damages every year (Borga et al., 2014;  
39 Cristiano et al., 2017; Paprotny et al., 2018). Physical laws translate increasing atmospheric  
40 temperature into increasing water vapor holding capacity. Together with changes in the  
41 atmospheric dynamics, this is expected to drive future precipitation changes (Trenberth et al.,  
42 2003; Pendergrass et al., 2020; Fowler et al., 2021b). In general, larger responses are expected for  
43 precipitation extremes because mean precipitation, on a global scale, is limited by energy  
44 constraints (Allan and Soden, 2008; Pendergrass & Hartmann, 2014). However, detecting  
45 changes in extreme precipitation is highly affected by the stochastic uncertainty characterizing  
46 the sampling of extremes. This uncertainty may mask the influence of climate forcing on the  
47 processes which locally control the extremes (Fatichi et al., 2016; Marra et al., 2019).

48 Statistically significant changes in the frequency of extreme precipitation in the past  
49 decades were reported, often with stronger trends in subdaily extremes, as opposed to daily  
50 (Guerreiro et al., 2018; Markonis et al., 2019; Papalexiou & Montanari, 2019). In some cases,  
51 opposing trends between short and long durations emerged, with complex implications for flood  
52 risk (Zheng et al., 2015). Available observations show different temporal trends for precipitation  
53 intensities associated to different exceedance probabilities (Schär et al., 2016; Pendergrass,  
54 2018). In general, increasing trends are reported for rarer events (Myhre et al., 2019), but the  
55 specific differences depend on duration, season, and local conditions, such as the dominating  
56 meteorological features contributing extremes (Blanchet et al., 2021; Moustakis et al., 2021).

57 Extreme return levels characterized by different exceedance probabilities are thus changing at  
58 different rates (Myhre et al., 2019; Marra et al., 2021).

59 Nonstationary extreme value models could aid the detection and quantification of trends  
60 in extreme precipitation of different exceedance probability (e.g., Min et al. 2009). However, the  
61 information these models can provide is impacted by stochastic uncertainties (Serinaldi and  
62 Kilsby, 2015; Fatichi et al., 2016), and their flexibility is limited by the assumptions concerning  
63 high order statistical moments. In fact, due to intrinsic limitations in parameter estimation  
64 accuracy, the shape (and sometimes also the scale) parameter of the extreme value distribution is  
65 usually assumed to be constant (Prosdocimi and Kjeldsen, 2021). Additionally, due to the  
66 structure of these statistical models, a link between the properties of the underlying process, such  
67 as precipitation occurrence frequency and intensity distribution, and extremes is difficult to  
68 establish (e.g. Marra et al., 2019). As such, the possibility to attribute the observed changes to  
69 specific physical and meteorological processes is hampered.

70 This background suggests that there is a need to move beyond traditional trend detection  
71 techniques applied to extremes only and develop novel methodologies. These methods should be  
72 able to detect general changes in extreme precipitation at multiple durations, quantify changes at  
73 different exceedance probabilities, and attribute these to changes in the underlying physical  
74 processes.

75 Miniussi and Marani (2020) proposed the so-called Metastatistical Extreme Value approach  
76 (Marani and Ignaccolo, 2015) as a viable way for addressing these issues. The idea relies on the  
77 concept of *ordinary events*, that is all the independent realizations of a process of interest, and  
78 proved highly effective in reducing stochasting uncertainties (Zorzetto et al., 2016; Marra et al.,  
79 2018). As opposed to traditional methods, the distribution describing the ordinary events is  
80 assumed to be known, and the extreme value distribution is derived by explicitly considering the  
81 occurrence frequency of the ordinary events. Miniussi and Marani (2020) provided an example  
82 application in which extreme return levels were computed over moving time windows,  
83 highlighting temporal changes that could not be appreciated using traditional methods. The  
84 adopted ordinary events (daily precipitation amounts), however, were not directly connected  
85 with meteorological systems, so that direct relations between changes in extremes and changes in  
86 the underlying storm properties is still missing.

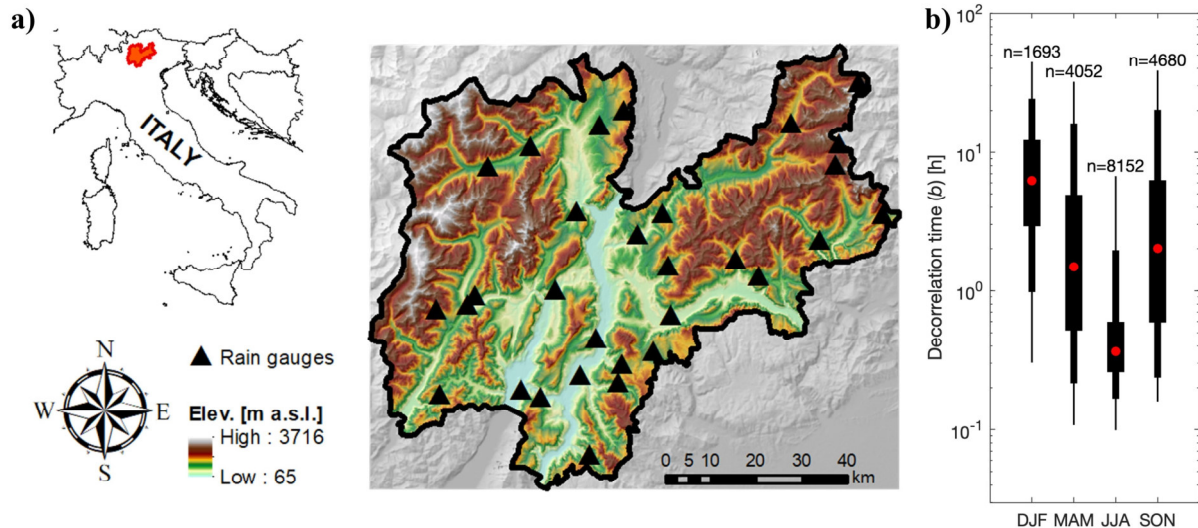
87 Here, we combine a novel approach for ordinary-events-based precipitation frequency  
88 analyses across durations (Marra et al., 2020) with a regional trend detection technique to: (a)  
89 detect and quantify trends in sub-daily annual maxima and extreme return levels by  
90 independently considering the changes in properties and occurrence frequency of storms, and (b)  
91 attribute the observed trends in extremes to specific changes in the local precipitation regime.  
92 We examine the relevant case of the eastern Italian Alps, where consistent significant changes in  
93 annual maximum precipitation intensities at subdaily and daily duration were reported (Libertino  
94 et al., 2019).

## 95 **2 Data and methodology**

### 96 **2.1 Study area and data**

97 We focus on Trentino, a 6000 km<sup>2</sup>-wide mountainous area in the Eastern Italian Alps  
98 (**Figure 1a**) which experienced significant increases in extreme short-duration rain intensities  
99 over the last decades (Libertino et al., 2019). Mean annual precipitation varies from ~1300 mm

100 yr<sup>-1</sup> in the south-eastern portion of the area to lower amounts (~900 mm yr<sup>-1</sup>) typical of the “inner  
 101 alpine province” in the north (Borga et al., 2005). A dense network of more than one hundred  
 102 rain gauges is present. From these, 30 stations (density ~1/200 km<sup>-2</sup>) with at least 27 complete  
 103 years (<10% missing data) of 5-minute resolution data in the period 1991-2020 are selected  
 104 (**Figure 1a**; see Table S1 in the Supporting Information).



105

106 **Figure 1. a)** Location and orography of the study area and location of the rain gauges used in  
 107 this study; **b)** Decorrelation time of the highest 25% ordinary events organized by season. The  
 108 red dots indicate the median values; bars indicates percentiles: 25-75th, 5-95th, 1-99th. The  
 109 number of storms occurred across the stations in each season is reported.

## 110 2.2 Definition of the ordinary events

111 Ordinary events are all the independent realizations of a process of interest, in our case  
 112 precipitation intensities at multiple durations. The here presented analysis is based on the storm-  
 113 based identification of ordinary events proposed by Marra et al. (2020), in which “storms” are  
 114 defined as independent meteorological objects, and “ordinary events” of each duration are  
 115 extracted from the storms. For each station, storms are defined as wet periods separated by dry  
 116 hiatuses of predefined length. We define as wet all the 5 min time intervals reporting at least 0.1  
 117 mm of precipitation, and separate storms using 24 hr dry hiatuses. A minimum duration of 30  
 118 min for a single storm is set to avoid individual tips to be considered as storms. Ordinary events  
 119 are then defined as the maximum intensities observed over the duration of interest in each storm  
 120 (details in Marra et al., 2020). Durations between 15 min to 24 hr are explored: 15 min, 30 min,  
 121 45 min, 1 h, 2 h, 3 h, 6 h, 12 h, 24h.

## 122 2.3 Tail of the ordinary events distribution

123 Previous studies show that subdaily precipitation intensities require three- (or more)  
 124 parameters distributions (Papalexiou et al., 2018). However, their right tails can be well  
 125 approximated using a two-parameter distribution which, in many cases, is found to be a Weibull  
 126 distribution (e.g., Zorzetto et al. 2016; Marra et al., 2020). This means that a portion of their  
 127 distribution including the extremes, which is here termed “tail”, can be approximated

128 as  $F(x; \lambda, \kappa) = 1 - e^{-\left(\frac{x}{\lambda}\right)^\kappa}$ , where  $\lambda$  is a scale parameter and  $\kappa$  is a shape parameter which  
 129 determines the tail heaviness. Larger shape parameters are associated to lighter tails, and vice  
 130 versa (see Figure S1). In particular, the tail is sub-exponential for  $\kappa > 1$ , exponential for  $\kappa=1$ , and  
 131 heavier than exponential for  $\kappa < 1$ .

132 The choice of the left-censoring threshold follows the test described in Marra et al.  
 133 (2020): the distribution parameters are estimated for different thresholds by censoring the values  
 134 below the left-censoring threshold as well as the observed annual maxima. The maxima are then  
 135 compared to the sampling confidence interval from the estimated distribution to assess whether  
 136 they could be likely samples. Following the method suggested in Marra et al. (2019), we select  
 137 the 75<sup>th</sup> percentile of the ordinary events for the left-censoring. This is in line with previous  
 138 findings in areas dominated by convective processes (Marra et al., 2019; Marra et al., 2020). It  
 139 should be recalled that the selection method implies a low sensitivity of the results to this  
 140 threshold.

#### 141 2.4 Extreme value model

142 The cumulative distribution  $\zeta(x)$  of extreme return levels  $x$  emerging from the  
 143 underlying distribution of ordinary events with tail  $F(x; \lambda, \kappa)$  can be written as  $\zeta(x) =$   
 144  $F(x; \lambda, \kappa)^n$ , where  $n$  is the average number of ordinary events per year (Marra et al., 2019;  
 145 Serinaldi et al., 2020). When one considers the  $j$ -th year of data, this formalism allows us to  
 146 quantify return levels from individual years by inverting  $\zeta_j(x) = F(x; \lambda_j, \kappa_j)^{n_j}$ , where  $\lambda_j$  and  $\kappa_j$   
 147 are the parameters describing the ordinary events tail at the  $j$ -th year and  $n_j$  is the number of  
 148 ordinary events in the year.

149 The parameters describing the ordinary events distribution tail are computed at each  
 150 station, duration and year by left-censoring the lowest 75% of the ordinary events and using the  
 151 least-squares method in Weibull-transformed coordinates (Marani and Ignaccolo, 2015). After  
 152 left-censoring, an average of  $\sim 14$  ordinary events per year (including annual maxima) are used  
 153 for parameter estimation. Yearly return levels are obtained by inverting the equation for  $\zeta_j(x)$ . In  
 154 this way, we obtain, for each station, yearly series of scale parameter, shape parameter, number  
 155 of ordinary events, and return levels. Annual maxima (AM) series are also extracted.

#### 156 2.5 Temporal trends analysis

157 We investigate the presence of monotonic trends in these quantities using the Regional  
 158 Mann-Kendall test at the 0.05 significance level (Mann, 1945; Kendall, 1975; Helsel & Frans,  
 159 2006), and we quantify the average rate of change using the nonparametric Sen's slope estimator  
 160 (Sen, 1968). Serial correlation in the series was tested and found negligible. In case trends within  
 161 the region are heterogeneous, the slope and significance estimated by the Regional Mann-  
 162 Kendall test could be misleading (Gilbert, 1987). We verify the homogeneity of the trends at the  
 163 different sites in the area by applying the Van Belle and Hughes test (1984). We find that  
 164 homogeneity is verified for all the investigated variables. As spatial correlation among nearby  
 165 stations could decrease the power of regional test, we include the correction proposed by Hirsch  
 166 and Slack (1984).

167 If the null hypothesis of the Mann-Kendall test is true (i.e., no trend) about half of the  
 168 pair comparisons between ordered data points is concordant and half discordant. . Considering

169 that 2 yr return levels correspond to the theoretical median of the AM, we consider the estimated  
170 trend on the 2 yr return levels as our model quantification of the trend in the AM.

## 171 2.6 Validation of the statistical model

172 The ability of our statistical model to reproduce observed trends in AM is verified by  
173 accounting for stochastic uncertainty in a Monte Carlo framework. For each station  $i$ , year  $j$  and  
174 duration  $d$ ,  $n_{ijd}$  Weibull-distributed ordinary events are generated according to the distribution  
175 parameters  $\lambda_{ijd}$  and  $\kappa_{ijd}$ , and the AM are extracted. The procedure is iterated 1000 times (which  
176 was found to provide coherent estimates of the 90% confidence interval), to obtain 1000  
177 synthetic regional sets of AM series for each duration. The Regional Mann-Kendall test is then  
178 performed on these sets to obtain 1000 slopes estimates for each duration, which provide a  
179 quantification of the stochastic uncertainty in the trends of the modelled AM. It is worth noting  
180 that this confidence interval is obtained by neglecting spatial correlation in the local exceedance  
181 probability of the events, and it is thus to be considered as a lower limit to the true confidence  
182 interval. In fact, such a correlation would cause a loss of information in the regional pooling of  
183 the trend test, inflating the stochastic uncertainty in the outcome.

## 184 2.7 Differential impact of ordinary events change on annual maxima changes

185 The relative impact of trends in the ordinary events characteristics and frequency on the  
186 emerging trend in the AM is evaluated. For each station and duration, the trends on modelled  
187 AM are computed using different combinations in which inter-annual variability in the  
188 parameters is either considered or ignored. In the latter case, the median parameter is used. We  
189 thus obtain the following cases: one case with 3 time-varying parameters (real case), 3  
190 combinations of 2 varying and 1 constant parameter, 3 combinations of 1 varying and 2 constant  
191 parameters, and one case of 3 constant parameters (no-change). Then the Regional Mann-  
192 Kendall test is applied to the resulting series.

## 193 2.8 Changes in the proportion of convective-like and other types of storms

194 Changes in the seasonal proportions between convective-like and other event types in  
195 different seasons are explored to investigate the seasonal and physical mechanisms underlying  
196 the observed trends. Events exceeding the left-censoring threshold at any of the durations are  
197 organized by seasons. The temporal decorrelation of the rain intensity timeseries is used as a  
198 proxy for broadly distinguishing between convective-like and other types of storms. The  
199 decorrelation time (**Figure 1b**) is taken equal to the scale parameter of the exponential fitting of  
200 the temporal autocorrelation. This is thus the time lag at which the temporal autocorrelation  
201 drops to  $e^{-1}$ . For each station and season, the yearly number of storms belonging to the two  
202 groups is calculated, and the significance and slope of the regional trend is estimated using the  
203 Regional Mann-Kendall test ( $p=0.05$ ) and the Sen's slope estimator. This shows if temporal  
204 changes in the proportion of different event types in the seasons emerged. A 2 hr threshold is  
205 found to optimally describe (that is, optimize the statistical significance) the temporal changes in  
206 our data and is therefore used as a proxy for distinguishing between convective-like  
207 (decorrelation time  $\leq 2$  hr) and other event types ( $> 2$  hr). Qualitatively analogous outcomes are  
208 obtained with thresholds between 1 and 3 hr.

## 209 3 Results and discussion

### 210 3.1 Regional trends on multi-duration extremes

211 Slopes for the regional trends for the nine investigated durations are reported in **Figure**  
212 **2a**. Hereinafter, slopes are normalized over the median value of each variable and expressed as  
213 percent change per year. As expected (Libertino et al., 2019), observed AM show positive trends  
214 at all durations. Statistically significant trends are observed for durations up to 6 hours and  
215 stronger increases for hourly and sub-hourly durations. The slopes estimated using the model  
216 (“modelled AM” in **Figure 2**) lie within the 90% confidence interval due to stochastic  
217 uncertainty (grey area), with the exception of the longest durations (12 and 24 h). Since at longer  
218 durations, the confidence interval is likely underestimated due to a larger correlation in the  
219 severity of the storms, this indicates that they are likely samples from our model. This means that  
220 the model well reproduces the trends in the observed AM.

221 The annual number of storms, uniquely defined for all durations (Marra et al., 2020),  
222 shows an increase ( $0.4\% \text{ yr}^{-1}$ ) (**Figure 2b**). Trends in the scale parameter of the intensity  
223 distributions are always positive, indicating a general increase in the intensity of the largest 25%  
224 of the ordinary events, with larger and significant increases (up to  $1.0\% \text{ yr}^{-1}$ ) for multi-hour  
225 durations (**Figure 2b**). The shape parameter shows negative trends for sub-hourly durations and  
226 positive trends for longer durations (**Figure 2b**), indicating that the proportion between heavy  
227 and mild events changed in different ways for short and long durations: increased tail heaviness  
228 is reported for sub-hourly durations and decreased tail heaviness for multi-hour durations (see  
229 Figure S1 for a visual interpretation of the effect of the shape parameter on tail-heaviness). At  
230 short durations the changes in the two parameters have a synergistic impact on extremes.  
231 Although the trend in individual parameters is not significant, observed and modelled AM  
232 experience stronger and significant changes. In contrast, at longer durations the changes in the  
233 parameters have opposing impact on extremes, and AM exhibit weaker increases, despite the  
234 increase of both scale parameter (significant) and yearly number of storms. In particular, where  
235 tail-heaviness has its strongest decrease (increase in the shape parameter), trends in extremes are  
236 at a minimum and are not significant.

237 These findings indicate that in the examined period (1991-2020) and area, AM exhibit  
238 significant changes, in particular for short-duration intensities, in agreement with previous  
239 studies (Libertino et al., 2019). Overall, our statistical model reproduces these trends accurately,  
240 and allows us to investigate the underlying statistical mechanisms. Changes in AM seem to be  
241 mostly influenced by changes in the tail-heaviness of the ordinary events, although trends in the  
242 shape parameter itself are not statistically significant.

### 243 3.2 Differential impact of ordinary events change on annual maxima changes

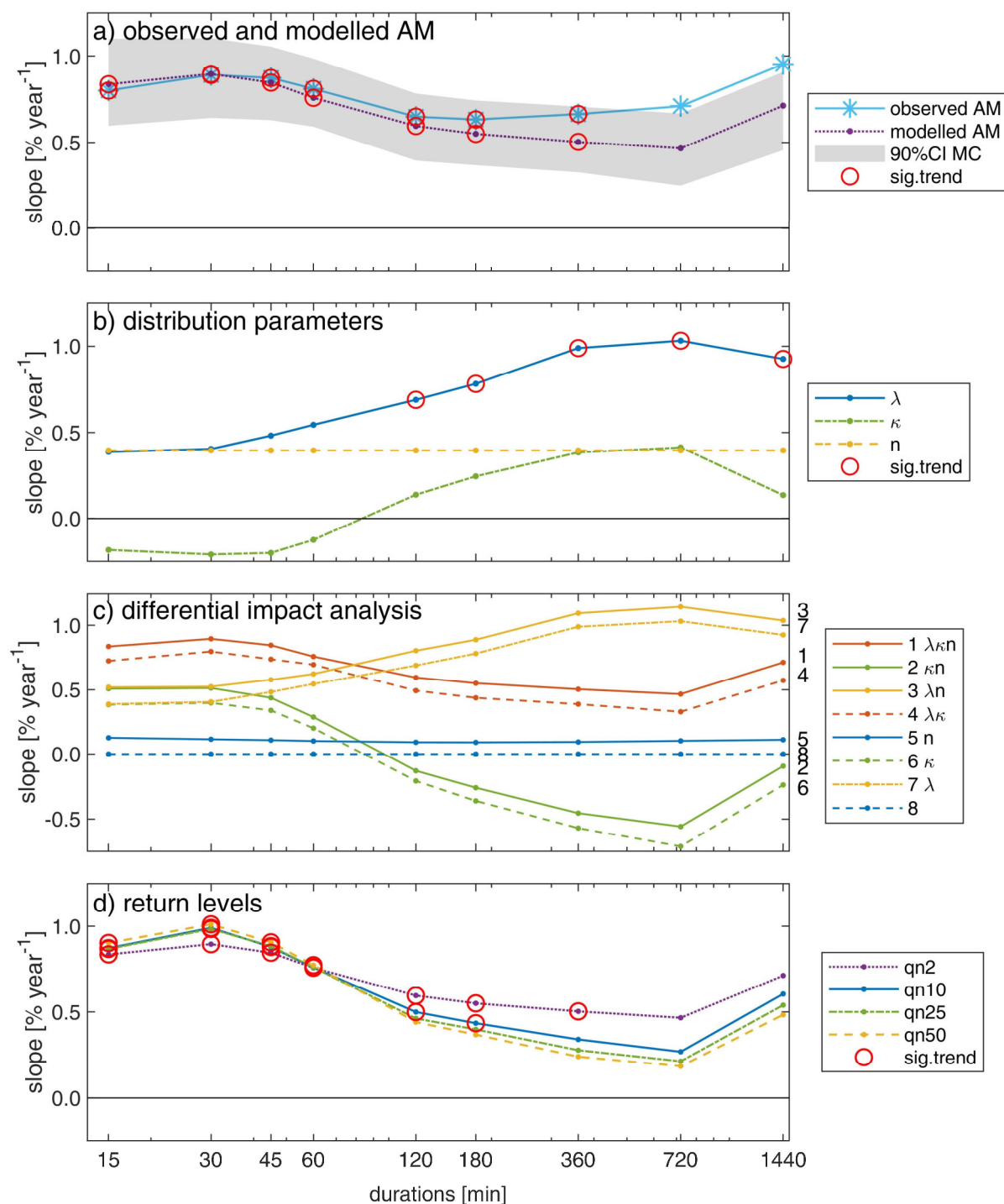
244 We investigate the impact of the trends in the individual model parameters on the trends  
245 in AM (**Figure 2c**). The ‘real’ case in which all parameters change with time reproduces the  
246 trends in the modelled AM (line 1 in **Figure 2c**). The other lines are a combination of varying  
247 and constant (median) parameters. Notably, the increase ( $+0.4\% \text{ yr}^{-1}$ ) in the number of yearly  
248 storms only has a marginal impact on the overall trends in extremes (same-color pairs of lines).  
249 Synergistic and opposing impacts of the other parameters are mostly evident by comparing the  
250 constant scale-parameter case (line 2) with the constant tail-heaviness case (line 3). When no  
251 changes in tail-heaviness are considered, AM show increasing trends whose magnitude can even

252 increase with duration, instead of decrease (lines 3, 7). This analysis shows that little changes in  
253 the tail-heaviness (shape parameter) turn into large changes in extreme intensities, suggesting  
254 this is an important parameter explaining the observed AM trends in the region. Crucially,  
255 without considering changes in tail heaviness it is not possible to explain the large observed  
256 increase in short-duration AM, as well as the different response of short and long duration  
257 extremes. This has profound implications for change-permitting extreme value models in which  
258 tail heaviness is often assumed to remain constant.

### 259 3.3 Regional trends of extreme return levels

260 Our statistical model allows to directly quantify changes on specific rare return levels. In  
261 general, slopes are always significantly positive for sub-hourly durations and decrease with  
262 increasing duration until they lose significance for durations above 2-3 hr (**Figure 2d**). For  
263 higher return levels, this behavior is enhanced: higher positive slopes are estimated for sub-  
264 hourly durations and lower not significant slopes for multi-hour durations. There is a duration  
265 interval between 1 and 2 hr where the trends don't depend on return period, closely following the  
266 change in regime in which the trend in the shape parameter crosses zero, that is no change in tail  
267 heaviness.

268 The here adopted statistical framework gives the opportunity to quantify and evaluate the  
269 statistical significance of trends in rare return levels of interest for hydrological design and risk  
270 management. It could be argued that estimating rare return levels on a yearly basis should lead to  
271 unberable uncertainties. We showed here that the statistical significance of trends in yearly-  
272 modelled return levels as high as the 50 yr events is comparable to the statistical significance of  
273 trends in AM, suggesting a similar signal to noise ratio. Trends on extreme return levels  
274 estimated on yearly basis from our model are thus characterized by stochastic uncertainties  
275 comparable to the ones of AM.



276

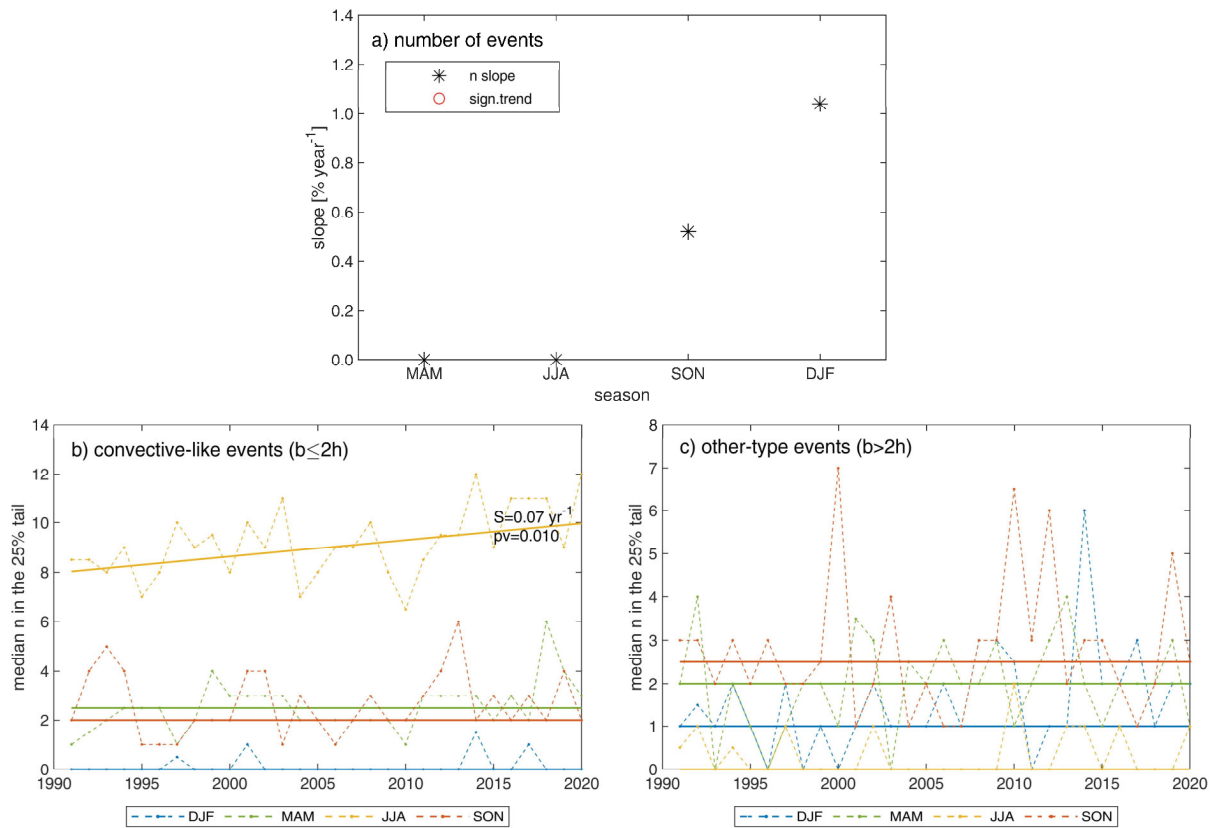
277 **Figure 2. a)** Slopes of the regional trends at different durations for observed and modelled AM;  
 278 significant trends ( $\alpha$ -level=0.05) are marked; stochastic uncertainty associated with the modelled  
 279 AM (90% C.I. of the MonteCarlo simulation) is also reported. **b)** Slopes of the regional trends  
 280 for the model parameters: scale parameter ( $\lambda$ ), shape parameter ( $\kappa$ ), and yearly number of storms  
 281 ( $n$ ); significant trends ( $\alpha$ -level=0.05) are marked. **c)** Differential impact on the modelled trends

282 of combinations of changes and no-changes in the model parameters; series labels report the  
283 parameters which are allowed to change. **d)** Slopes of the regional trends for some estimated  
284 return levels (2, 10, 25, 50 yr); significant trends ( $\alpha$ -level=0.05) are marked; note that the 2 yr  
285 return levels correspond to the modelled AM.

### 286 3.4 Changes in the proportion of convective-like events

287 The parametrization of our model allows us to formulate hypotheses about the physical  
288 processes underlying the detected changes. In particular, the observed changes could be  
289 explained by an increased number of intense convective events, which would mainly contribute  
290 to the short duration annual maxima. We analyze possible changes in the number of storms  
291 occurring in different seasons, and in the seasonal number of convective-like and other types of  
292 storms (**Figure 3**). The positive trend in the yearly number of storms reported above is fully  
293 explained by the increases in the number of storms in autumn (SON, **Figure 3a**) and in winter  
294 (DJF). However, examining changes in the types composition shows no distinct increase in  
295 convective-like storms during these seasons (**Figure 3b, c**).

296 Conversely, although no trend emerges in the number of storms in summer (JJA), the  
297 number of summer convective-like storms in this season increased significantly, while the  
298 number of other storms shows no trend (**Figure 3b, c**). This implies a significant increase in the  
299 proportion of summer convective-like events. Since convective-like storms are generally  
300 associated with heavy intensities at short durations, this change in composition could explain the  
301 observed increase in tail heaviness at short durations, and thus the observed trends on short-  
302 duration AM. This is confirmed when the parameters of the ordinary events distribution are  
303 examined considering spring-summer (MAMJJA) and autumn-winter (SONDJF) separately  
304 (**Figure S2**). These results suggest that the significant positive trends found for short-duration  
305 extremes are mostly related to changes in summer storms, and that these can be related to  
306 changes in the intensity distributions (increasing tail-heaviness) induced by an increasing  
307 proportion of heavy convective-like storms in the summer.



308

309 **Figure 3. a)** Slope of the regional trends for the number of seasonal storms; significant trends  
 310 ( $\alpha$ -level=0.05) are marked. **b)** Median (across stations) seasonal number of convective-like  
 311 (decorrelation time  $\leq 2$  hr) and **c)** other (decorrelation time  $> 2$  hr) storms in the 25% tail; the  
 312 Sen's slope (S) and the p-value (pv) of the Regional Mann-Kendall test are reported in case of  
 313 significant trends ( $\alpha$ -level=0.05).

### 314 5 Conclusions

315 We examine changes in extreme sub-daily precipitation intensities for the relevant case of  
 316 the eastern Italian Alps, where consistent significant changes in annual maximum (AM)  
 317 intensities were reported (Libertino et al., 2019). Specifically, we aim at detecting and  
 318 quantifying trends in sub-daily AM and extreme return levels, and linking the observed trends in  
 319 extremes to specific changes in the local precipitation regime. To do so, we adopt a novel unified  
 320 framework for extreme value analyses based on ordinary events, and we quantify trends by  
 321 means of the regional Mann-Kendall test. With respect to traditional change-permitting extreme  
 322 value models, the here presented method provides a statistical tool for better quantifying changes  
 323 in extremes in spite of the large stochastic uncertainties, and for better understanding the  
 324 observed changes by separately considering multi-duration storm intensity distributions and  
 325 storm occurrence frequency.

326 Results confirm the presence of significant positive trends in the AM. Trends in the 2 yr  
 327 return levels estimated yearly using our model are consistent with the observed trends in AM.  
 328 These trends are more marked for 15 min to 1 hr durations and less marked for 3 hr to 24 hr

329 durations. The model parametrization allows to conclude that these trends are likely due to a  
330 combination of (i) increasing number of storm events per year and increasing intensity of the  
331 storms, and (ii) changes in the tail properties of the storms. In particular, an increasing, albeit  
332 not-significant, trend in tail heaviness at short durations seems to mostly explain the changes in  
333 AM and return levels. A significant increase in the proportion of convective-like storms is  
334 detected during the summer (JJA). This could explain the observed trends in AM and return  
335 levels emerged at the short durations in this study. This agrees with results reported by Fowler et  
336 al. (2021a), who highlight that the stronger increases in short-duration extremes are related to  
337 feedbacks in convective clouds dynamics at the local scale. The approach can be expanded to  
338 directly consider different types of storm events (Marra et al., 2019), following previous works  
339 regarding mixed distributions like the Two-component Extreme value distribution (Rossi et al.,  
340 1984) or the mixed Gumbel (Kjeldsen et al., 2018).

341 The trends in this study are derived from a relatively short data series and should be  
342 considered as representative of the examined period only (1991-2020). Due to decadal climate  
343 variability, they should not be considered as representative of climate change in general, nor  
344 extrapolated to predict future conditions (Iliopoulou and Koutsoyiannis, 2020). Nevertheless,  
345 our approach could provide insights for better describing local climatologies under change, and  
346 for enhancing our understanding of the linkages with changes in the underlying physical  
347 processes. This information can be valuable for improving our ability to create and use process-  
348 based change-permitting statistical models for hydrometeorological extremes.

#### 349 **Data Availability Statement**

350 Precipitation data was provided by the Provincia Autonoma di Trento and can be  
351 retrieved from <https://www.meteotrentino.it> (Last accessed: September 2021). The codes used  
352 for the statistical model are available at <https://doi.org/10.5281/zenodo.3971558>. The Regional  
353 Mann-Kendall trend test was performed based on the functions by J. Burkey, downloaded from  
354 <https://it.mathworks.com/matlabcentral/fileexchange/22389-seasonal-kendall-test-with-slope-for-serial-dependent-data> (retrieved July 2021). The codes developed in the study and the elaborated  
355 data for reproducing the results of the paper are available at  
356 <https://www.dropbox.com/sh/f7cf93racbg5hqv/AADXBHHTKebd5OtG9syKrIJOa?dl=0> for the  
357 purpose of peer review and, upon acceptance, will be made publicly available in their final  
358 version.  
359

#### 360 **CRedit authors' contribution**

361 **ED:** Data curation, Methodology, Formal analysis, Investigation, Visualization, Writing –  
362 original draft, Writing – review & editing. **MB:** Conceptualization, Investigation, Writing –  
363 review & editing, Supervision. **MZ:** Visualization, Writing – review & editing. **FM:**  
364 Conceptualization, Methodology, Software, Investigation, Writing – original draft, Writing –  
365 review & editing, Supervision.

#### 366 **Acknowledgements**

367 The authors declare no conflict of interests. This study was funded by Provincia  
368 Autonoma di Trento through Accordo di Programma GPR. FM thanks the Institute of  
369 Atmospheric Sciences and Climate (ISAC), National Research Council of Italy for the support.

370 **References**

- 371 Alexander, L. V., N. Tapper, X. Zhang, H. J. Fowler, C. Tebaldi, and A. Lynch (2009), Climate  
372 extremes: Progress and future directions, *Int. J. Climatol.*, 29, 317–319.
- 373 Allan, R. P., Soden, B. J., 2008. Atmospheric Warming and the Amplification of Precipitation  
374 Extremes. *Science*, 321, 5895, 1481-1484. <https://doi.org/10.1126/science.1160787>
- 375 Blanchet J., Creutin JD., Blanc A. (2021). Retreating winter and strengthening autumn  
376 Mediterranean influence on extreme precipitation in the Southwestern Alps over the last  
377 60 years. *Environ. Res. Lett.* 16 034056, <https://doi.org/10.1088/1748-9326/abb5cd>
- 378 Borga M., Vezzani C. & Fontana G.D. (2005). Regional Rainfall Depth–Duration–Frequency  
379 Equations for an Alpine Region. *Nat Hazards* 36, 221–235.  
380 <https://doi.org/10.1007/s11069-004-4550-y>
- 381 Chen Y., Paschalis A., Kendon E., Kim D., Onof C. (2021). Changing spatial structure of  
382 summer heavy rainfall, using convection-permitting ensemble. *Geophysical Research*  
383 *Letters*, 48, e2020GL090903. <https://doi.org/10.1029/2020GL090903>
- 384 Chow, V. T., Maidment, D. R., & Mays, L. W. (1988). *Applied hydrology*. McGraw-Hill
- 385 Cristiano, E., ten Veldhuis, M.-C., and van de Giesen, N. (2017). Spatial and temporal variability  
386 of rainfall and their effects on hydrological response in urban areas – a review, *Hydrol.*  
387 *Earth Syst. Sci.*, 21, 3859–3878, <https://doi.org/10.5194/hess-21-3859-2017>
- 388 Fatichi, S., Ivanov, V. Y., Paschalis, A., Peleg, N., Molnar, P., Rimkus, S., et al. (2016).  
389 Uncertainty partition challenges the predictability of vital details of climate change.  
390 *Earth's Future*, 4, 240–251. <https://doi.org/10.1002/2015EF000336>
- 391 Fischer RA, Tippett LHC. (1928). Limiting forms of the frequency distribution of the largest or  
392 smallest member of a sample. *Math Proc Camb Philos Soc* 1928;24(02):180–90.
- 393 Fowler H.J., Lenderink G., Prein, A.F. et al. (2021a) Anthropogenic intensification of short-  
394 duration rainfall extremes. *Nat Rev Earth Environ* 2, 107–122.  
395 <https://doi.org/10.1038/s43017-020-00128-6>
- 396 Fowler H. J., et al. (2021b). Towards advancing scientific knowledge of climate change impacts  
397 on short-duration rainfall extremes. *Phil. Trans. R. Soc. A* 379: 20190542.  
398 <https://doi.org/10.1098/rsta.2019.0542>
- 399 Gilbert, R. O. (1987). *Statistical methods for environmental pollution monitoring*. New York  
400 City: Wiley. <https://doi.org/10.2307/1270090>
- 401 Gnedenko B. (1943). Sur la distribution limite du terme maximum d'une serie aleatoire. *Ann*  
402 *Math* 1943;44(3):423–53.
- 403 Groisman P.Ya., Knight R.W., Easterling D.R., Karl T.R., Hegerl G.C., Razuvaev V.N. (2005).  
404 Trends in intense precipitation in the climate record. (2005) *Journal of Climate*, 18 (9),  
405 pp. 1326-1350. Cited 935 times. doi: 10.1175/JCLI3339.1
- 406 Guerreiro, S.B., Fowler, H.J., Barbero, R. et al. (2018). Detection of continental-scale  
407 intensification of hourly rainfall extremes. *Nature Clim Change* 8, 803–807.  
408 <https://doi.org/10.1038/s41558-018-0245-3>

- 409 Haerter, J. O., P. Berg, and S. Hagemann (2010), Heavy rain intensity distributions on varying  
 410 time scales and at different temperatures, *J. Geophys. Res.*, 115, D17102,  
 411 doi:10.1029/2009JD013384
- 412 Helsel, D. R., & Frans, L. M. (2006). Regional Kendall test for trend. *Environmental Science &*  
 413 *Technology*, 40(13), 4066–4073.
- 414 Hirsch, R. M.; Slack, J. R. (1984). A nonparametric trend test for seasonal data with serial  
 415 dependence. *Water Resour. Res.* 1984, 20, 727-732
- 416 Iliopoulou T, Koutsoyiannis D. (2020). Projecting the future of rainfall extremes: Better classic  
 417 than trendy. *J. Hydrol.*, 588 , p. 125005, <https://doi.org/10.1016/j.jhydrol.2020.125005>.
- 418 Kendall, M. G. (1975). *Rank Correlation Methods*. New York, NY: Oxford University Press.
- 419 Kjeldsen, T. R., Ahn, H., Prosdocimi I., Heo J. (2018) Mixture Gumbel models for extreme  
 420 series including infrequent phenomena, *Hydrological Sciences Journal*, 63:13-14, 1927-  
 421 1940, DOI: 10.1080/02626667.2018.1546956
- 422 Lenderink, G., and E. van Meijgaard (2008), Increase in hourly precipitation extremes beyond  
 423 expectations from temperature changes, *Nat. Geosci.*, 1, 511–514.
- 424 Libertino A., Ganora D., & Claps P. (2019). Evidence for increasing rainfall extremes remains  
 425 elusive at large spatial scales: The case of Italy. *Geophysical Research Letters*, 46, 7437–  
 426 7446. <https://doi.org/10.1029/2019GL083371>
- 427 Mann, H. B. (1954) Non-parametric tests against trend. *Econometrica* 1945, 13, 245-259.
- 428 Marani M., Ignaccolo M. (2015). A metastatistical approach to rainfall extremes, *Advances in*  
 429 *Water Resources*, Volume 79, 2015, Pages 121-126, ISSN 0309-1708,  
 430 <https://doi.org/10.1016/j.advwatres.2015.03.001>.
- 431 Marchi L., Borga M., Preciso E., Gaume E. (2010). Characterisation of selected extreme flash  
 432 floods in Europe and implications for flood risk management. *J. Hydrol.*, 394, pp. 118-  
 433 133, <https://doi.org/10.1016/j.jhydrol.2010.07.017>
- 434 Markonis, Y., Papalexiou, S. M., Martinkova, M., & Hanel, M. (2019). Assessment of water cycle  
 435 intensification over land using a multi source global gridded precipitation dataset. *Journal*  
 436 *of Geophysical Research: Atmospheres*, <https://doi.org/10.1029/2019JD030855>
- 437 Marra, F., Armon, M., Adam, O., Zoccatelli, D., Gazal, O., Garfinkel, C. I., et al. (2021).  
 438 Towards narrowing uncertainty in future projections of local extreme precipitation.  
 439 *Geophysical Research Letters*, 48, e2020GL091823.  
 440 <https://doi.org/10.1029/2020GL091823>
- 441 Marra, F., Nikolopoulos, E. I., Anagnostou, E. N., & Morin, E. (2018). Metastatistical extreme  
 442 value analysis of hourly rainfall from short records: Estimation of high quantiles and  
 443 impact of measurement errors. *Advances in Water Resources*, 117, 27–39.  
 444 <https://doi.org/10.1016/j.advwatres.2018.05.001>
- 445 Marra, F., Zoccatelli, D., Armon, M., & Morin, E. (2019). A simplified MEV formulation to  
 446 model extremes emerging from multiple nonstationary underlying processes. *Advances in*  
 447 *Water Resources*, 127, 280–290. <https://doi.org/10.1016/j.advwatres.2019.04.002>

- 448 Marra, F., Borga, M., & Morin, E. (2020). A unified framework for extreme subdaily  
 449 precipitation frequency analyses based on ordinary events. *Geophysical Research Letters*,  
 450 47, e2020GL090209.
- 451 Min SK, Zhang X, Zwiers F, Friederichs P, Hense A (2009) Signal detectability in extreme  
 452 precipitation changes assessed from twentieth century climate simulations. *Clim Dyn*  
 453 32:95–111
- 454 Miniussi, A., & Marani, M. (2020). Estimation of daily rainfall extremes through the  
 455 metastatistical extreme value distribution: Uncertainty minimization and implications for  
 456 trend detection. *Water Resources Research*, 56, e2019WR026535.  
 457 <https://doi.org/10.1029/2019WR026535>
- 458 Miniussi, A., Villarini, G., & Marani, M. (2020). Analyses through the metastatistical extreme  
 459 value distribution identify contributions of tropical cyclones to rainfall extremes in the  
 460 eastern United States. *Geophysical Research Letters*, 47, e2020GL087238.  
 461 <https://doi.org/10.1029/2020GL087238>
- 462 Moustakis, Y., Papalexiou, S. M., Onof, C. J., & Paschalis, A. (2021). Seasonality, intensity, and  
 463 duration of rainfall extremes change in a warmer climate. *Earth's Future*, 9,  
 464 e2020EF001824. <https://doi.org/10.1029/2020EF001824>
- 465 Myhre, G., Alterskjær, K., Stjern, C.W. et al. Frequency of extreme precipitation increases  
 466 extensively with event rareness under global warming. *Sci Rep* 9, 16063 (2019).  
 467 <https://doi.org/10.1038/s41598-019-52277-4>
- 468 Papalexiou, S. M., AghaKouchak, A., & Foufoula-Georgiou, E. (2018). A diagnostic framework  
 469 for understanding climatology of tails of hourly precipitation extremes in the United  
 470 States. *Water Resources Research*, 54(9), 6725–6738.  
 471 <https://doi.org/10.1029/2018WR022732>
- 472 Papalexiou, S. M., & Montanari, A. (2019). Global and regional increase of precipitation  
 473 extremes under global warming. *Water Resources Research*, 55, 4901–4914.  
 474 <https://doi.org/10.1029/2018WR024067>
- 475 Paprotny, D., Sebastian, A., Morales-Napoles, O., & Jonkman, S. N. (2018). Trends in flood  
 476 losses in Europe over the past 150 years. *Nature Communications*, 9, 1985
- 477 Pendergrass, A. G. (2018). What precipitation is extreme? *Science*, 360, 6393.  
 478 <https://doi.org/10.1126/science.aat1871>
- 479 Pendergrass, A.G. (2020). Changing Degree of Convective Organization as a Mechanism for  
 480 Dynamic Changes in Extreme Precipitation. *Curr Clim Change Rep* 6, 47–54.  
 481 <https://doi.org/10.1007/s40641-020-00157-9>
- 482 Pendergrass, A. G., Hartman, D. L. (2014). The Atmospheric Energy Constraint on Global-Mean  
 483 Precipitation Change. *J. Climate*, 27, 2, 757-768, [https://doi.org/10.1175/JCLI-D-13-](https://doi.org/10.1175/JCLI-D-13-00163.1)  
 484 00163.1
- 485 Prosdocimi, I., Kjeldsen, T. Parametrisation of change-permitting extreme value models and its  
 486 impact on the description of change. *Stoch Environ Res Risk Assess* 35, 307–324 (2021).  
 487 <https://doi.org/10.1007/s00477-020-01940-8>

- 488 Rossi, F., Fiorentino, M., and Versace, P. (1984), Two-Component Extreme Value Distribution  
489 for Flood Frequency Analysis, *Water Resour. Res.*, 20( 7), 847– 856,  
490 doi:10.1029/WR020i007p00847.
- 491 Schär C., N. Ban, E.M. Fischer, et al., 2016. Percentile indices for assessing changes in heavy  
492 precipitation events. *Clim. Change*, 137, 201-216, [https://doi.org/10.1007/s10584-016-](https://doi.org/10.1007/s10584-016-1669-2)  
493 [1669-2](https://doi.org/10.1007/s10584-016-1669-2)
- 494 Sen PK (1968). Estimates of the regression coefficient based on Kendall's tau, *J. Am. Statist.*  
495 *Assoc.*, 63, 1379–1389, <http://doi.org/10.1080/01621459.1968.10480934>
- 496 Serinaldi, F., & Kilsby, C. G. (2015). Stationarity is undead: Uncertainty dominates the  
497 distribution of extremes. *Advances in Water Resources*, 77, 17–36.
- 498 Trenberth, K. E., A. Dai, R. M. Rasmussen, and D. B. Parsons (2003), The changing character of  
499 precipitation, *Bull. Am. Meteorol. Soc.*, 84, 1205– 1217.
- 500 van Belle G., Hughes, J. P. (1984) Nonparametric tests for trend in water quality. *Water Resour.*  
501 *Res.* 1984, 20, 127-136.
- 502 Zheng F., Westra S., Leonard M. (2015). Opposing local precipitation extremes. *Nature Clim*  
503 *Change* 5, 389–390. <https://doi.org/10.1038/nclimate2579>
- 504 Zorzetto E., Botter G., Marani M. (2016). On the emergence of rainfall extremes from ordinary  
505 events. *Geophysical Research Letters*, 43, 8076–8082.  
506 <https://doi.org/10.1002/2016GL069445>